



Contents lists available at ScienceDirect

European Journal of Medicinal Chemistry

journal homepage: <http://www.elsevier.com/locate/ejmech>

Research paper

Dehydrodieugenol B derivatives as antiparasitic agents: Synthesis and biological activity against *Trypanosoma cruzi*

Daiane D. Ferreira ^{a,1}, Fernanda S. Sousa ^{b,1}, Thais A. Costa-Silva ^c, Juliana Q. Reimão ^d, Ana C. Torrecilhas ^b, Deidre M. Johns ^e, Claire E. Sear ^f, Kathia M. Honorio ^g, João Henrique G. Lago ^c, Edward A. Anderson ^{f,**}, Andre G. Tempone ^{a,*}

^a Centre for Parasitology and Mycology, Instituto Adolfo Lutz, São Paulo, 01246-000, Brazil

^b Institute of Environmental, Chemical and Pharmaceutical Sciences, Federal University of São Paulo, Diadema, 09972-270, Brazil

^c Center of Natural and Human Sciences, Federal University of ABC, Santo André, 09210-580, Brazil

^d Faculdade de Medicina de Jundiaí, Rua Francisco Telles, 250 Vila Arens II 13202550, Jundiaí, SP, Brazil

^e Department of Biomedical Sciences, Carlson College of Veterinary Medicine, Oregon State University, Corvallis, OR, 97331, USA

^f Chemistry Research Laboratory, University of Oxford, 12 Mansfield Road, Oxford, OX1 3TA, UK

^g Escola de Artes, Ciências e Humanidades, Universidade de São Paulo, São Paulo, 03828-000, Brazil

ARTICLE INFO

Article history:

Received 26 February 2019

Received in revised form

30 April 2019

Accepted 1 May 2019

Available online 2 May 2019

Keywords:

Neolignans

Drugs

Therapy

Trypanosoma cruzi

Chagas disease

ABSTRACT

Chagas disease is a neglected protozoan disease that affects more than eight million people in developing countries. Due to the limited number and toxicity profiles of therapies in current use, new drugs are urgently needed. In previous studies, we reported the isolation of two related antitrypanosomal neolignans from *Nectandra leucantha* (Lauraceae). In this work, a semi-synthetic library of twenty-three neolignan derivatives was prepared to explore synthetically accessible structure activity relationships (SAR) against *Trypanosoma cruzi*. Five compounds demonstrated activity against trypomastigotes (IC₅₀ values from 8 to 64 μM) and eight showed activity against intracellular amastigotes (IC₅₀ values from 7 to 16 μM). Eighteen derivatives demonstrated no mammalian cytotoxicity up to 200 μM. The phenolic acetate derivative of natural dehydrodieugenol B was effective against both parasite forms and eliminated 100% of amastigotes inside macrophages. This compound caused rapid and intense depolarization of the mitochondrial membrane potential, with decreased levels of intracellular reactive oxygen species being observed. Fluorescence assays demonstrated that this derivative affected neither the permeability nor the electric potential of the parasitic plasma membrane, an effect also corroborated by scanning electron microscopy studies. Structure-activity relationship studies (SARs) demonstrated that the presence of at least one allyl side chain on the biaryl ether core was important for antitrypanosomal activity, and that the free phenol is not essential. This set of neolignan derivatives represents a promising starting point for future Chagas disease drug discovery studies.

© 2019 Elsevier Masson SAS. All rights reserved.

1. Introduction

Chagas disease is a major public health issue in Latin America, where it is endemic in more than twenty countries [1,2]. Migrant populations, and modes of transmission such as blood, food and organ donation, have further led to the spread of this disease to

Europe, North America, Japan and Australia [3–5]. Approximately eight million people are infected worldwide, causing approximately 7000 deaths annually [6,7]. Current treatments for Chagas disease comprise two nitro-substituted heterocyclic drugs, benznidazole and nifurtimox [8]. These compounds have shown successful clinical, parasitological, and serological treatment outcomes during the acute phase and in congenital Chagas disease [9]. However, these drugs are far from ideal: efficacy diminishes with disease chronification [10], and both exhibit undesirable toxicity profiles leading to adverse side-effects. Furthermore, parasite resistance to these treatments is becoming more frequent [11–13]. Collectively, these facts highlight an urgent need for safer and more

* Corresponding author.

** Corresponding author.

E-mail addresses: edward.anderson@chem.ox.ac.uk (E.A. Anderson), andre.tempone@ial.sp.gov.br, atempone@usp.br (A.G. Tempone).¹ These authors contributed equally to the work.

Abbreviations

ANOVA	analysis of variance
BALB/c	isogenic murine lineage
CCCP	carbonylcyanidem-chlorophenylhydrazone
CC ₅₀	50% cytotoxic concentration
DiSBAC2(3)	bis-(1,3-diethylthiobarbituric acid) trimethine oxonol
DMAP	4-dimethylaminopyridine
DMF	dimethylformamide
DMSO	dimethylsulfoxide
FDA	Food and Drug Administration
FBS	fetal bovine serum
H2DCF-DA	2,7 -dichlorodihydrofluorescein diacetate
HBSS	Hank's Balanced Salt Solution
HPLC	high performance liquid chromatography
HRESIMS	high resolution electrospray ionization mass spectra
IC ₅₀	50% inhibitory concentration

JC-1	5,5,6,6-tetrachloro-1,1,3,3-tetraethylbenzimidazole carbocyanide iodide
LLCMK2	Kidney Rhesus monkey cells
MS	mass spectrometry
MTT	3-(4,5-dimethylthiazol-2-yl)-2,5-diphenyltetrazolium bromide
NCTC	cells-clone L929, murine conjunctive cells
NMR	nuclear magnetic resonance
PAINS	Pan-Assay Interference Compounds
PBS	phosphate buffered saline
ROS	reactive oxygen species
RPMI-1640	Roswell Park Memorial Institute medium
SAR	structure activity relationships
SI	selectivity index
SYTOX [®]	Green amino(4-(6-(amino(iminio)methyl)-1Hindol-2-yl) phenyl) methaniminium chloride
TLC	thin layer chromatography
THF	tetrahydrofuran
TMS	tetramethylsilane

efficacious drugs.

Natural products are a proven source of new chemical scaffolds for drug discovery, as evidenced by the large number of FDA-approved drugs that are derived from or are inspired by natural products [14]. Compounds isolated from the *Nectandra* genus (Lauraceae), have been shown to exhibit antibacterial, anti-inflammatory, arterial hypertension control, antitumor, and anti-parasitic activity [15]. We recently reported the first phytochemical study of *Nectandra leucantha*, which led to the isolation of the neolignans dehydrodieugenol B (**1**) and methyldehydrodieugenol B (**2**) (Fig. 1). These compounds were found to display bioactivity against the intracellular forms of *Leishmania donovani* [16] and *Trypanosoma cruzi* [17]. In light of these results, and due to the urgent need for novel bioactive lead compounds for drug development against Chagas disease, we performed a semi-synthetic derivatization of compounds **1** and **2** to explore the effects of structural modifications on their biological activity. Here we describe the results of these studies, which involved the preparation of 23 semi-synthetic derivatives, and evaluation of their anti-parasitic activity against *Trypanosoma cruzi*, and their mammalian cytotoxicity. Of these derivatives, compound **14** (see below) was selected for phenotypic studies of drug-treated parasites to identify possible target organelles.

2. Material and methods

2.1. General experimental procedures

NMR spectra were recorded on a Bruker AVIIIHD 400 nanobay spectrometer, operating at 400 and 101 MHz for ¹H and ¹³C nuclei, respectively. CDCl₃ was used as solvent with tetramethylsilane as internal standard, or by reference to the residual solvent peak (δ_{H}

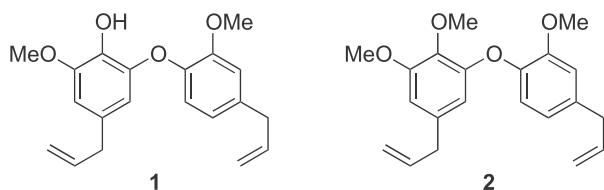


Fig. 1. Structures of compounds **1** and **2** isolated from *Nectandra leucantha*.

7.26; δ_{C} 77.10 ppm). Chemical shifts (δ) are reported in ppm and coupling constants (J) in Hz. High resolution electrospray ionization mass spectra (HRESIMS) were obtained using a Bruker Daltonics MicroTOF-Q IITM ESI-Qq-TOF in positive mode. Silica gel 60 (Merck, 63–210 mesh) was used for the column chromatographic separation procedures, while silica gel 60 PF₂₅₄ (Merck) was used for TLC (0.25 mm). For all extraction and chromatography procedures, analytical grade solvents were used.

2.2. Isolation of compounds **1** and **2** from *N. leucantha* leaves

As described previously [18], the *n*-hexane extract from twigs of *N. leucantha* (7.4 g) was subjected to successive column chromatography over silica gel and Sephadex LH-20 to afford compounds **1** (1.58 g) and **2** (1.15 g) in 99% purity as indicated by HPLC.

2.3. Hydrogenation procedures for preparation of compounds **3** and **25**

2.3.1. 2-Methoxy-6-(2-methoxy-4-propylphenoxy)-4-propylphenol (**3**)

To a solution of compound **1** (0.30 mmol) in EtOH (5 mL) was added 10% wt Pd/C (0.09 mmol). The reaction flask was purged with hydrogen and the reaction mixture was stirred for 1 h under H₂ (1 atm). After filtration through Celite[®], the filtrate was concentrated under reduced pressure to afford compounds **3** (98.7 mg, 0.29 mmol, 99%) as a yellow oil; ¹H NMR (CDCl₃) δ_{H} 6.87 (1H, d, J = 8.1 Hz), 6.79 (1H, d, J = 1.9 Hz), 6.69 (1H, dd, J = 8.1 and 1.9 Hz), 6.48 (1H, d, J = 1.9 Hz), 6.40 (1H, d, J = 1.9 Hz), 5.85 (1H, s, OH), 3.89 (3H, s), 3.87 (3H, s), 2.60–2.52 (2H, m), 2.49–2.39 (2H, m), 1.70–1.60 (2H, m), 1.60–1.50 (2H, m), 0.95 (3H, t, J = 7.3 Hz), 0.89 (3H, t, J = 7.3 Hz). ¹³C NMR (CDCl₃) δ_{C} 150.2, 147.6, 144.3, 143.9, 139.1, 134.8, 133.8, 120.7, 119.3, 112.8, 111.7, 107.1, 56.2, 56.0, 37.9, 37.8, 24.7, 24.7, 13.9, 13.7. HRESIMS m/z 353.1720 [M+Na]⁺ (calc. for C₂₀H₂₆NaO₄ 353.1723).

2.3.2. 1,2-Dimethoxy-3-(2-methoxy-4-propylphenoxy)-5-propylbenzene (**25**)

To a solution of compounds **2** (0.088 mmol) in EtOH (2 mL) was added 10% wt Pd/C (0.028 mmol). The reaction flask was purged with hydrogen and the reaction mixture was stirred for 1 h under H₂ (1 atm). After filtration through Celite[®], the filtrate was

concentrated under reduced pressure to afford compound **25** (36.0 mg, 0.104 mmol, 98%) as a yellow oil; ^1H NMR (CDCl_3) δ_{H} 6.78 (2H, m), 6.68 (1H, dd, $J = 8.1$ and 1.8 Hz), 6.47 (1H, d, $J = 1.8$ Hz), 6.26 (1H, d, $J = 1.8$ Hz), 3.87 (6H, s), 3.83 (3H, s), 2.61–2.50 (2H, m), 2.48–2.37 (2H, m), 1.65 (2H, m), 1.59–1.47 (2H, m), 0.95 (3H, t, $J = 7.3$ Hz), 0.88 (3H, t, $J = 7.3$ Hz). ^{13}C NMR (CDCl_3) δ_{C} 153.3, 150.5, 150.4, 143.8, 138.7, 138.2, 137.7, 120.6, 119.2, 112.9, 111.2, 107.1, 61.0, 56.1, 56.0, 38.1, 37.9, 24.7, 24.5, 13.9, 13.8. HRESIMS m/z 367.1876 $[\text{M}+\text{Na}]^+$ (calc. for $\text{C}_{21}\text{H}_{28}\text{NaO}_4$ 367.1880).

2.4. Alkylation procedure for preparation of compounds 4–13

To a suspension of NaH (3.6 mg, 60% wt, 0.090 mmol) in DMF (300 μL) at 0 °C was added compound **1** or **3** (0.060 mmol). To this solution was added the respective alkyl halide (see specific procedure for quantities) via microsyringe, and the resulting mixture was stirred at 0 °C for 2 h. After addition of saturated aq. NH_4Cl (1 mL) and extraction using EtOAc (3×1 mL), the organic layers were washed with H_2O (4×1 mL), brine (1 mL) and dried over MgSO_4 . After concentration under reduced pressure, the crude product was purified by flash column chromatography on silica gel (petroleum ether/EtOAc, 8:2) to afford the alkylated products **4–13**.

2.4.1. 5-Allyl-1-(4-allyl-2-methoxyphenoxy)-2-ethoxy-3-methoxybenzene (**4**)

Prepared from **1** using ethyl iodide (0.10 mmol, 1.7 equiv.) as electrophile. Yellow oil, 18.1 mg, 0.051 mmol, 85% yield; ^1H NMR (CDCl_3) δ_{H} 6.80–6.77 (2H, m), 6.68 (1H, dd, $J = 8.1, 1.9$ Hz), 6.48 (1H, d, $J = 1.9$ Hz), 6.30 (1H, d, $J = 1.9$ Hz), 6.04–5.83 (2H, m), 5.13–4.99 (4H, m), 4.08 (2H, q, $J = 7.1$ Hz), 3.85 (3H, s), 3.83 (3H, s), 3.36 (2H, d, $J = 6.7$ Hz), 3.24 (2H, d, $J = 6.7$ Hz), 1.28 (3H, t, $J = 7.1$ Hz). ^{13}C NMR (CDCl_3) δ_{C} 153.8, 150.7, 150.4, 144.4, 137.5, 137.1, 137.0, 135.7, 135.4, 120.7, 119.1, 115.9, 115.8, 113.0, 111.7, 107.4, 69.1, 56.1, 56.0, 40.1, 39.9, 15.5. HRESIMS m/z 377.1719 $[\text{M}+\text{Na}]^+$ (calc. for $\text{C}_{22}\text{H}_{26}\text{NaO}_4$ 377.1723).

2.4.2. 5-Allyl-1-(4-allyl-2-methoxyphenoxy)-3-methoxy-2-propoxybenzene (**5**)

Prepared from **1** using *n*-propyl iodide (0.10 mmol, 1.7 equiv.) as electrophile. Yellow oil, 21.1 mg, 0.057 mmol, 95%; ^1H NMR (CDCl_3) δ_{H} 6.78 (1H, d, $J = 1.8$ Hz), 6.75 (1H, d, $J = 8.1$ Hz), 6.67 (1H, dd, $J = 8.1, 1.8$ Hz), 6.49 (1H, d, $J = 1.8$ Hz), 6.33 (1H, d, $J = 1.8$ Hz), 6.03–5.83 (2H, m), 5.13–4.99 (4H, m), 3.96 (2H, t, $J = 6.7$ Hz), 3.85 (3H, s), 3.84 (3H, s), 3.36 (2H, d, $J = 6.7$ Hz), 3.25 (2H, d, $J = 6.7$ Hz), 1.68 (2H, sextet, $J = 7.5$ Hz), 0.90 (3H, t, $J = 7.5$ Hz). ^{13}C NMR (CDCl_3) δ_{C} 153.8, 150.4, 150.2, 144.6, 137.5, 137.5, 137.1, 135.5, 135.3, 120.7, 118.7, 115.9, 115.8, 112.9, 112.1, 107.6, 75.2, 56.1, 56.0, 40.1, 39.9, 23.3, 10.3. HRESIMS m/z 391.1877 $[\text{M}+\text{Na}]^+$ (calc. for $\text{C}_{23}\text{H}_{28}\text{NaO}_4$ 391.1880).

2.4.3. 5-Allyl-1-(4-allyl-2-methoxyphenoxy)-2-butoxy-3-methoxybenzene (**6**)

Prepared from **1** using *n*-butyl iodide (0.10 mmol, 1.7 equiv.) as electrophile. Yellow oil, 26.4 mg, 0.069 mmol, 97%; ^1H NMR (CDCl_3) δ_{H} 6.79 (1H, d, $J = 1.9$ Hz), 6.75 (1H, d, $J = 8.1$ Hz), 6.68 (1H, dd, $J = 8.1, 1.9$ Hz), 6.49 (1H, d, $J = 1.9$ Hz), 6.33 (1H, d, $J = 1.9$ Hz), 6.04–5.83 (2H, m), 5.13–5.00 (4H, m), 3.99 (2H, t, $J = 6.7$ Hz), 3.84 (3H, s), 3.84 (3H, s), 3.36 (2H, d, $J = 6.7$ Hz), 3.25 (2H, d, $J = 6.7$ Hz), 1.68–1.59 (2H, m), 1.36 (2H, sextet, $J = 7.5$ Hz), 0.87 (3H, t, $J = 7.5$ Hz). ^{13}C NMR (CDCl_3) δ_{C} 153.8, 150.4, 150.2, 144.6, 137.6, 137.5, 137.2, 135.5, 135.3, 120.7, 118.6, 115.9, 115.8, 112.9, 112.1, 107.6, 73.3, 56.1, 56.0, 40.1, 40.0, 32.1, 19.0, 13.9. HRESIMS m/z 405.2030 $[\text{M}+\text{Na}]^+$ (calc. for $\text{C}_{24}\text{H}_{30}\text{NaO}_4$ 405.2036).

2.4.4. 5-Allyl-1-(4-allyl-2-methoxyphenoxy)-2-(allyloxy)-3-methoxybenzene (**7**)

Prepared from **1** using allyl bromide (0.12 mmol, 2.0 equiv.) as electrophile. Yellow oil, 21.9 mg, 0.059 mmol, 99%; ^1H NMR (CDCl_3) δ_{H} 6.79 (1H, d, $J = 8.1$ Hz), 6.79 (1H, d, $J = 1.9$ Hz), 6.69 (1H, dd, $J = 8.1$ and 1.9 Hz), 6.48 (1H, d, $J = 1.9$ Hz), 6.29 (1H, d, $J = 1.9$ Hz), 6.11–5.81 (3H, m), 5.24 (1H, dq, $J = 17.2$ and 1.5 Hz), 5.15–4.99 (5H, m), 4.55 (2H, dt, $J = 6.0$ and 1.5 Hz), 3.85 (3H, s), 3.83 (3H, s), 3.37 (2H, d, $J = 6.7$ Hz), 3.24 (2H, d, $J = 6.7$ Hz). ^{13}C NMR (CDCl_3) δ_{C} 153.8, 150.7, 150.5, 144.3, 137.4, 137.1, 136.7, 135.8, 135.6, 134.6, 120.7, 119.2, 117.4, 115.9, 115.8, 113.1, 111.5, 107.4, 74.3, 56.1, 56.0, 40.1, 40.0. HRESIMS m/z 389.1720 $[\text{M}+\text{Na}]^+$ (calc. for $\text{C}_{23}\text{H}_{26}\text{NaO}_4$ 389.1723).

2.4.5. 5-Allyl-1-(4-allyl-2-methoxyphenoxy)-2-(benzyloxy)-3-methoxybenzene (**8**)

Prepared from **1** using benzyl bromide (0.087 mmol, 1.45 equiv.) as electrophile. Yellow oil, 24.2 mg, 0.058 mmol, 96%; ^1H NMR (CDCl_3) δ_{H} 7.40–7.36 (2H, m), 7.28–7.25 (3H, m), 6.79–6.74 (2H, m), 6.69 (1H, d, $J = 1.9$ Hz), 6.49 (1H, d, $J = 1.9$ Hz), 6.33 (1H, d, $J = 1.9$ Hz), 6.03–5.85 (2H, m), 5.14–5.00 (6H, m), 3.82 (3H, s), 3.80 (3H, s), 3.36 (2H, d, $J = 6.7$ Hz), 3.25 (2H, d, $J = 6.7$ Hz). ^{13}C NMR (CDCl_3) δ_{C} 153.8, 150.6, 150.4, 144.4, 138.0, 137.5, 137.1, 137.0, 135.7, 128.3, 128.0, 127.8, 127.6, 120.8, 119.0, 115.9, 115.8, 113.0, 111.8, 107.6, 75.0, 56.1, 56.0, 40.1, 40.0. HRESIMS m/z 439.1877 $[\text{M}+\text{Na}]^+$ (calc. for $\text{C}_{27}\text{H}_{28}\text{NaO}_4$ 439.1880).

2.4.6. 2-Ethoxy-1-methoxy-3-(2-methoxy-4-propylphenoxy)-5-propylbenzene (**9**)

Prepared from **3** using ethyl iodide (0.10 mmol, 1.7 equiv.) as electrophile. Pale yellow oil, 19.7 mg, 0.055 mmol, 92%; ^1H NMR (CDCl_3) δ_{H} 6.78 (1H, d, $J = 1.9$ Hz), 6.76 (1H, d, $J = 8.1$ Hz), 6.66 (1H, dd, $J = 8.1$ and 1.9 Hz), 6.47 (1H, d, $J = 1.9$ Hz), 6.29 (1H, d, $J = 1.9$ Hz), 4.08 (2H, q, $J = 7.1$ Hz), 3.85 (3H, s), 3.84 (3H, s), 2.59–2.52 (2H, m), 2.48–2.40 (2H, m), 1.70–1.61 (2H, m), 1.59–1.50 (2H, m), 1.27 (3H, t, $J = 7.1$ Hz), 0.95 (3H, t, $J = 7.3$ Hz), 0.89 (3H, t, $J = 7.3$ Hz). ^{13}C NMR (CDCl_3) δ_{C} 153.6, 150.6, 150.2, 144.1, 138.4, 138.1, 136.7, 120.6, 118.9, 112.9, 111.5, 107.3, 69.0, 56.1, 56.0, 38.0, 37.8, 24.7, 24.5, 15.5, 13.9, 13.8. HRESIMS m/z 381.2036 $[\text{M}+\text{Na}]^+$ (calc. for $\text{C}_{22}\text{H}_{30}\text{NaO}_4$ 381.2036).

2.4.7. 1-Methoxy-3-(2-methoxy-4-propylphenoxy)-2-propoxy-5-propylbenzene (**10**)

Prepared from **3** using *n*-propyl iodide (0.10 mmol, 1.7 equiv.) as electrophile. Yellow oil, 19.0 mg, 0.051 mmol, 85%; ^1H NMR (CDCl_3) δ_{H} 6.78 (1H, d, $J = 1.9$ Hz), 6.73 (1H, d, $J = 8.1$ Hz), 6.65 (1H, dd, $J = 8.1$ and 1.9 Hz), 6.48 (1H, d, $J = 1.9$ Hz), 6.32 (1H, d, $J = 1.9$ Hz), 3.95 (2H, t, $J = 6.8$ Hz), 3.85 (3H, s), 3.84 (3H, s), 2.59–2.51 (2H, m), 2.48–2.41 (2H, m), 1.72–1.60 (4H, m), 1.59–1.50 (2H, m), 0.94 (3H, t, $J = 7.3$ Hz), 0.93 (3H, t, $J = 7.3$ Hz), 0.89 (3H, t, $J = 7.3$ Hz). ^{13}C NMR (CDCl_3) δ_{C} 153.6, 150.3, 150.0, 144.3, 138.1, 138.0, 137.2, 120.5, 118.4, 112.8, 111.9, 107.5, 75.2, 56.1, 56.0, 38.0, 37.8, 24.7, 24.5, 23.3, 13.8, 13.8, 10.3. HRESIMS m/z 395.2190 $[\text{M}+\text{Na}]^+$ (calc. for $\text{C}_{23}\text{H}_{32}\text{NaO}_4$ 395.2193).

2.4.8. 2-Butoxy-1-methoxy-3-(2-methoxy-4-propylphenoxy)-5-propylbenzene (**11**)

Prepared from **3** using *n*-butyl iodide (0.10 mmol, 1.7 equiv.) as electrophile. Yellow oil, 18.2 mg, 0.047 mmol, 78%; ^1H NMR (CDCl_3) δ_{H} 6.78 (1H, d, $J = 1.9$ Hz), 6.72 (1H, d, $J = 8.1$ Hz), 6.65 (1H, dd, $J = 8.1$ and 1.9 Hz), 6.48 (1H, d, $J = 1.9$ Hz), 6.32 (1H, d, $J = 1.9$ Hz), 3.98 (2H, t, $J = 6.7$ Hz), 3.84 (6H, s), 2.58–2.53 (2H, m), 2.47–2.42 (2H, m), 1.68–1.61 (4H, m), 1.59–1.51 (2H, m), 1.41–1.31 (2H, m), 0.95 (3H, t, $J = 7.3$ Hz), 0.95 (3H, t, $J = 7.3$ Hz), 0.87 (3H, t, $J = 7.3$ Hz). ^{13}C NMR (CDCl_3) δ_{C} 153.6, 150.2, 150.0, 144.3, 138.1, 138.0, 137.2, 120.5, 118.4, 112.8, 111.9, 107.5, 73.3, 56.1, 56.0, 38.0, 37.8, 32.1, 24.7,

24.5, 19.0, 13.9, 13.8, 13.8. HRESIMS m/z 409.2345 $[M+Na]^+$ (calc. for $C_{24}H_{34}NaO_4$ 409.2349).

2.4.9. 2-(Allyloxy)-1-methoxy-3-(2-methoxy-4-propylphenoxy)-5-propylbenzene (**12**)

Prepared from **3** using allyl bromide (0.12 mmol, 2.0 equiv.) as electrophile. Pale yellow oil, 19.2 mg, 0.052 mmol, 86%; 1H NMR ($CDCl_3$) δ_H 6.80–6.75 (2H, m), 6.67 (1H, dd, $J = 8.1$ and 1.9 Hz), 6.47 (1H, d, $J = 1.9$ Hz), 6.28 (1H, d, $J = 1.9$ Hz), 6.10–5.98 (1H, m), 5.23 (1H, dq, $J = 17.2$ and 1.5 Hz), 5.11 (1H, ddd, $J = 10.3$, 2.9 and 1.1 Hz), 4.54 (2H, dt, $J = 6.0$ and 1.5 Hz), 3.85 (3H, s), 3.83 (3H, s), 2.59–2.53 (2H, m), 2.46–2.41 (2H, m), 1.64 (2H, sextet, $J = 7.4$ Hz), 1.54 (2H, sextet, $J = 7.4$ Hz), 0.95 (3H, t, $J = 7.4$ Hz), 0.88 (3H, t, $J = 7.4$ Hz). ^{13}C NMR ($CDCl_3$) δ_C 153.6, 150.5, 150.3, 144.0, 138.5, 138.3, 136.4, 134.7, 120.6, 119.0, 117.3, 113.0, 111.3, 107.2, 74.2, 56.1, 56.0, 38.0, 37.8, 24.7, 24.5, 13.9, 13.8. HRESIMS m/z 393.2034 $[M+Na]^+$ (calc. for $C_{23}H_{30}NaO_4$ 393.2036).

2.4.10. 2-(Benzyloxy)-1-methoxy-3-(2-methoxy-4-propylphenoxy)-5-propylbenzene (**13**)

Prepared from **3** using benzyl bromide (0.10 mmol, 1.7 equiv.) as electrophile. Pale yellow oil, 19.9 mg, 0.048 mmol, 80%; 1H NMR ($CDCl_3$) δ_H 7.39–7.37 (2H, m), 7.28–7.26 (3H, m), 6.77 (1H, d, $J = 1.9$ Hz), 6.74 (1H, d, $J = 8.1$ Hz), 6.66 (1H, dd, $J = 8.1$ and 1.9 Hz), 6.48 (1H, d, $J = 1.9$ Hz), 6.33 (1H, d, $J = 1.9$ Hz), 5.04 (2H, s), 3.83 (3H, s), 3.80 (3H, s), 2.59–2.53 (2H, m), 2.48–2.43 (2H, m), 1.70–1.61 (2H, m), 1.61–1.51 (2H, m), 0.96 (3H, t, $J = 7.3$ Hz), 0.89 (3H, t, $J = 7.3$ Hz). ^{13}C NMR ($CDCl_3$) δ_C 153.7, 150.4, 150.1, 144.2, 138.4, 138.4, 138.0, 136.7, 128.3, 128.0, 127.5, 120.6, 118.7, 112.9, 111.7, 107.5, 75.0, 56.1, 55.9, 38.1, 37.9, 24.7, 24.5, 13.9, 13.8. HRESIMS m/z 443.2191 $[M+Na]^+$ (calc. for $C_{27}H_{32}NaO_4$ 443.2193).

2.5. Acetylation procedure for preparation of compounds 14 and 15

Compounds **1** or **3** (0.060 mmol), acetic anhydride (0.45 mmol) and pyridine (1.38 mmol) were heated to $100^\circ C$ for 2 h. The cooled mixture was diluted with iced H_2O , acidified dropwise with 1 M HCl and extracted with EtOAc (3×1 mL). The combined organic extracts were dried over $MgSO_4$ and concentrated under reduced pressure. The crude product was purified by flash chromatography (petroleum ether/EtOAc, 8:2), to afford products **14** and **15**, respectively.

2.5.1. 4-Allyl-2-(4-allyl-2-methoxyphenoxy)-6-methoxyphenyl acetate (**14**)

Prepared from **1**; Yellow oil, 21.2 mg, 0.058 mmol, 96%; 1H NMR ($CDCl_3$) δ_H 6.87 (1H, d, $J = 8.1$ Hz), 6.79 (1H, d, $J = 1.9$ Hz), 6.70 (1H, dd, $J = 8.1$ and 1.9 Hz), 6.50 (1H, d, $J = 1.9$ Hz), 6.26 (1H, d, $J = 1.9$ Hz), 6.04–5.81 (2H, m), 5.14–5.00 (4H, m), 3.82 (3H, s), 3.81 (3H, s), 3.37 (2H, d, $J = 6.7$ Hz), 3.26 (2H, d, $J = 6.7$ Hz), 2.25 (3H, s). ^{13}C NMR ($CDCl_3$) δ_C 168.7, 152.3, 150.9, 150.2, 143.5, 138.4, 137.3, 136.8, 136.8, 128.5, 121.0, 120.6, 116.2, 116.0, 113.1, 110.5, 106.7, 56.1, 56.1, 40.2, 40.0, 20.5. HRESIMS m/z 391.1518 $[M+Na]^+$ (calc. for $C_{22}H_{24}NaO_5$ 391.1516).

2.5.2. 2-Methoxy-6-(2-methoxy-4-propylphenoxy)-4-propylphenyl acetate (**15**)

Prepared from **3**; yellow oil, 19.7 mg, 0.053 mmol, 62%; 1H NMR ($CDCl_3$) δ_H 6.84 (1H, d, $J = 8.1$ Hz), 6.78 (1H, d, $J = 1.9$ Hz), 6.68 (1H, dd, $J = 8.1$ and 1.9 Hz), 6.48 (1H, d, $J = 1.9$ Hz), 6.25 (1H, d, $J = 1.9$ Hz), 3.82 (3H, s), 3.82 (3H, s), 2.60–2.52 (2H, m), 2.48–2.42 (2H, m), 2.24 (3H, s), 1.70–1.60 (2H, m), 1.58–1.49 (2H, m), 0.95 (3H, t, $J = 7.3$ Hz), 0.89 (3H, t, $J = 7.3$ Hz). ^{13}C NMR ($CDCl_3$) δ_C 168.8, 152.1, 150.7, 150.1, 143.2, 141.1, 139.4, 128.1, 120.8, 120.4, 113.1, 110.4, 106.6, 56.1, 56.1, 38.3, 37.9, 24.6, 24.4, 20.5, 13.8, 13.8. HRESIMS m/z 395.1826

$[M+Na]^+$ (calc. for $C_{22}H_{28}NaO_5$ 395.1829).

2.6. Propionylation procedure for preparation of compounds 16 and 17

2.6.1. 4-Allyl-2-(4-allyl-2-methoxyphenoxy)-6-methoxyphenyl propionate (**16**)

To a solution of **1** (23.7 mg, 0.071 mmol) in 120 μL of CH_2Cl_2 at $0^\circ C$ were added Et_3N (19 μL , 0.14 mmol), DMAP (0.8 mg, 0.007 mmol) and propionyl chloride (6.2 μL , 0.071 mmol). The reaction mixture was allowed to warm to room temperature and was stirred for 3 h. After concentration under reduced pressure, the resulting oily residue was redissolved in EtOAc (1 mL), washed with H_2O and the aqueous phase extracted with EtOAc (4×1 mL). The combined organic phases were dried over $MgSO_4$, filtered and evaporated to dryness under reduced pressure. The crude product was purified by flash chromatography (petroleum ether/EtOAc, 8:2), to afford **16** (17.5 mg, 0.046 mmol, 64%) as a pale yellow oil; 1H NMR ($CDCl_3$) δ_H 6.85 (1H, d, $J = 8.1$ Hz), 6.78 (1H, d, $J = 1.8$ Hz), 6.69 (1H, dd, $J = 8.1$ and 1.8 Hz), 6.50 (1H, d, $J = 1.8$ Hz), 6.29 (1H, d, $J = 1.8$ Hz), 6.03–5.81 (2H, m), 5.14–5.00 (4H, m), 3.81 (6H, s), 3.36 (2H, d, $J = 6.7$ Hz), 3.26 (2H, d, $J = 6.7$ Hz), 2.53 (2H, q, $J = 7.5$ Hz), 1.18 (3H, t, $J = 7.5$ Hz). ^{13}C NMR ($CDCl_3$) δ_C 172.1, 152.4, 150.8, 150.1, 143.7, 138.2, 137.3, 136.8, 136.5, 128.7, 120.9, 120.3, 116.2, 115.9, 113.1, 110.9, 106.9, 56.2, 56.1, 40.2, 40.0, 27.1, 9.2. HRESIMS m/z 405.1669 $[M+Na]^+$ (calc. for $C_{23}H_{26}NaO_5$ 405.1672).

2.6.2. 2-Methoxy-6-(2-methoxy-4-propylphenoxy)-4-propylphenyl propionate (**17**)

To a solution of **3** (20 mg, 0.06 mmol) in 120 μL of CH_2Cl_2 at $0^\circ C$ were added Et_3N (16 μL , 0.12 mmol), DMAP (0.7 mg, 0.006 mmol) and propionyl chloride (5.8 μL , 0.066 mmol). The reaction mixture was allowed to warm to room temperature and was stirred for 3 h. After concentration under reduced pressure, the resulting oily residue was redissolved in EtOAc (1 mL), washed with H_2O and the aqueous phase extracted with EtOAc (4×1 mL). The combined organic phases were dried over $MgSO_4$, filtered and evaporated to dryness under reduced pressure. The crude product was purified by flash chromatography (petroleum ether/EtOAc, 8:2), to afford **17** (14.3 mg, 0.037 mmol, 56%) as a yellow oil; 1H NMR ($CDCl_3$) δ_H 6.82 (1H, d, $J = 8.1$ Hz), 6.77 (1H, d, $J = 1.9$ Hz), 6.67 (1H, dd, $J = 8.1$ and 1.9 Hz), 6.49 (1H, d, $J = 1.9$ Hz), 6.28 (1H, d, $J = 1.9$ Hz), 3.82 (6H, s), 2.58–2.54 (2H, m), 2.54–2.50 (2H, m), 2.50–2.43 (2H, m), 1.69–1.60 (2H, m), 1.59–1.50 (2H, m), 1.17 (3H, t, $J = 7.3$ Hz), 0.95 (3H, t, $J = 7.3$ Hz), 0.89 (3H, t, $J = 7.3$ Hz). ^{13}C NMR ($CDCl_3$) δ_C 172.1, 152.2, 150.6, 149.9, 143.5, 140.9, 139.1, 128.4, 120.8, 120.0, 113.1, 110.7, 106.8, 56.1, 56.1, 38.2, 37.8, 27.1, 24.7, 24.4, 13.8, 13.8, 9.2. HRESIMS m/z 409.1984 $[M+Na]^+$ (calc. for $C_{23}H_{30}NaO_5$ 409.1985).

2.7. Isomerization procedure for preparation of compounds 18 and 22

2.7.1. 2-Methoxy-6-(2-methoxy-4-prop-1-en-1-yl)phenoxy)-4-prop-1-en-1-yl)phenol (**18**)

A solution of **1** (50 mg, 0.153 mmol) and KOH (85 mg, 1.53 mmol) in ethylene glycol (200 μL) was refluxed at $150^\circ C$ for 16 h. The reaction mixture was cooled to room temperature, diluted with H_2O and extracted with EtOAc (4×1 mL). The combined organic extracts were washed with H_2O (3×1 mL), brine (1 mL), dried over $MgSO_4$ and concentrated under reduced pressure. The crude product was purified by flash chromatography (petroleum ether/EtOAc, 7:3), to afford **18** (33.2 mg, 0.102 mmol, 66% yield) as a yellow oil. A mixture of diastereomers (5:1) was formed at each alkene. Data is reported for the major (*E,E*) diastereomer, which was assigned by analogy to literature precedents. 1H NMR ($CDCl_3$) δ_H

6.95 (1H, d, $J = 1.8$ Hz), 6.89 (1H, d, $J = 8.2$ Hz), 6.84 (1H, dd, $J = 8.2$ and 1.8 Hz), 6.66 (1H, d, $J = 1.8$ Hz), 6.53 (1H, d, $J = 1.8$ Hz), 6.40–6.31 (1H, m), 6.25–6.12 (2H, m), 6.06–5.95 (1H, m), 3.91 (3H, s), 3.87 (3H, s), 1.88 (3H, dd, $J = 6.6$ and 1.5 Hz), 1.81 (3H, dd, $J = 6.6$ and 1.5 Hz). ^{13}C NMR (CDCl_3) δ_{C} 153.6, 150.5, 144.7, 144.5, 135.9, 134.7, 130.5, 130.4, 129.6, 129.4, 125.3, 124.1, 119.6, 109.7, 109.4, 104.3, 56.2, 56.0, 18.4, 18.3. HRESIMS m/z 349.1407 $[\text{M}+\text{Na}]^+$ (calc. for $\text{C}_{20}\text{H}_{22}\text{NaO}_4$ 349.1410).

2.7.2. 1,2-Diethoxy-3-(2-methoxy-4-prop-1-en-1-yl)phenoxy)-5-prop-1-en-1-yl)benzene (**22**)

A solution of **2** (50 mg, 0.146 mmol) and KOH (81 mg, 1.46 mmol) in ethylene glycol (200 μL) was refluxed at 150°C for 16 h. The reaction mixture was cooled to room temperature, diluted with H_2O and extracted with EtOAc (4×1 mL). The combined organic extracts were washed with H_2O (3×1 mL), brine (1 mL), dried over MgSO_4 and concentrated under reduced pressure. The crude product was purified by flash chromatography (petroleum ether/EtOAc, 7:3), to afford **22** (49 mg, 0.144 mmol, 98%) as a pale yellow oil. A mixture of diastereomers (5:1) was formed at each alkene. Data is reported for the major (*E,E*) diastereomer, which was assigned by analogy to literature precedents, and by a coupling constant of 15.7 Hz for one of the alkene protons. ^1H NMR (CDCl_3) δ_{H} 6.96 (1H, d, $J = 1.9$ Hz), 6.86–6.80 (2H, m), 6.64 (1H, d, $J = 1.9$ Hz), 6.41 (1H, d, $J = 1.9$ Hz), 6.37 (1H, dd, $J = 15.7$ and 1.9 Hz), 6.25–6.13 (2H, m), 6.11–5.97 (1H, m), 3.89 (3H, s), 3.87 (3H, s), 3.85 (3H, s), 1.88 (3H, dd, $J = 6.6$ and 1.5 Hz), 1.81 (3H, dd, $J = 6.5$ and 1.5 Hz). ^{13}C NMR (CDCl_3) δ_{C} 153.7, 150.7, 150.7, 144.9, 138.9, 134.4, 133.7, 130.6, 130.5, 125.6, 125.2, 119.7, 118.7, 110.0, 109.0, 104.6, 61.2, 56.2, 56.1, 18.6, 18.4. HRESIMS m/z 363.1563 $[\text{M}+\text{Na}]^+$ (calc. for $\text{C}_{21}\text{H}_{24}\text{NaO}_4$ 363.1567).

2.8. Hydroboration/oxidation procedure for preparation of compounds 19 and 23

2.8.1. 4-(3-Hydroxypropyl)-2-(4-(3-hydroxypropyl)-2-methoxyphenoxy)-6-methoxyphenol (**19**)

To a stirred solution of **1** (25 mg, 0.076 mmol) in THF (200 μL) under argon was added $\text{BH}_3\cdot\text{THF}$ (152 μL , 1 M in THF, 0.152 mmol). After 2 h, 3 M NaOH (150 μL , 0.23 mmol) and H_2O_2 (160 μL , 30% aq., 0.76 mmol) were added, and the reaction mixture was stirred at room temperature for 1.5 h. Brine (1 mL) was added, and the product was extracted with EtOAc (3×1 mL). The organic layer was washed with brine (1 mL), dried over MgSO_4 and the solvent removed under reduced pressure. The crude product was purified by flash chromatography (petroleum ether/EtOAc 1:1 and 3:7) to afford **19** (22 mg, 0.061 mmol, 80%) as a pale yellow oil; ^1H NMR (CDCl_3) δ_{H} 6.86 (1H, d, $J = 8.1$ Hz), 6.81 (1H, d, $J = 1.8$ Hz), 6.71 (1H, dd, $J = 8.1$ and 1.8 Hz), 6.50 (1H, d, $J = 1.8$ Hz), 6.38 (1H, d, $J = 1.8$ Hz), 3.89 (3H, s), 3.86 (3H, s), 3.68 (2H, t, $J = 6.4$ Hz), 3.62 (2H, t, $J = 6.4$ Hz), 2.72–2.64 (2H, m), 2.60–2.51 (2H, m), 1.95–1.85 (2H, m), 1.84–1.75 (2H, m), 1.26 (1H, d, $J = 6.2$ Hz, OH), 1.19 (1H, d, $J = 6.2$ Hz, OH). ^{13}C NMR (CDCl_3) δ_{C} 150.3, 147.8, 144.4, 144.0, 138.3, 135.0, 132.9, 120.7, 119.5, 112.8, 111.4, 107.1, 62.2, 62.1, 56.2, 56.0, 34.3, 34.2, 31.9, 31.8. HRESIMS m/z 385.1618 $[\text{M}+\text{Na}]^+$ (calc. for $\text{C}_{20}\text{H}_{26}\text{NaO}_6$ 385.1622).

2.8.2. 1-(4-(5-(1-Hydroxypropyl)-2,3-dimethoxyphenoxy)-3-methoxyphenyl)propan-1-ol (**23**). To a stirred solution of **22** (25 mg, 0.073 mmol) in THF (200 μL) under argon was added $\text{BH}_3\cdot\text{THF}$ (146 μL , 1 M in THF, 0.146 mmol)

After 2 h, 3 M NaOH (140 μL , 0.22 mmol) and H_2O_2 (180 μL , 30% aq., 0.73 mmol) were added, and the reaction mixture was stirred at room temperature for 1.5 h. Brine (1 mL) was added, and the product was extracted with EtOAc (3×1 mL). The organic layer was

washed with brine (1 mL), dried over MgSO_4 and the solvent removed under reduced pressure. The crude product was purified by flash chromatography (petroleum ether/EtOAc 1:1 and 3:7) to afford **23** (22 mg, 0.058 mmol, 80%, unassigned mixture of stereoisomers) as a yellow oil; ^1H NMR (CDCl_3) δ_{H} 6.99 (1H, s), 6.80 (2H, s), 6.69 (1H, d, $J = 1.7$ Hz), 6.41 (1H, d, $J = 1.7$ Hz), 4.56 (1H, t, $J = 6.6$ Hz), 4.43 (1H, t, $J = 6.6$ Hz), 3.89 (3H, s), 3.86 (3H, s), 3.85 (3H, s), 1.76–1.59 (4H, m), 1.25 (1H, d, $J = 6.2$ Hz, OH), 1.19 (1H, d, $J = 6.2$ Hz, OH), 0.92 (3H, t, $J = 7.4$ Hz), 0.86 (3H, t, $J = 7.4$ Hz). ^{13}C NMR (CDCl_3) δ_{C} 153.7, 150.6, 150.2, 145.1, 140.6, 140.3, 119.2, 118.9, 118.4, 110.2, 109.2, 104.6, 75.8, 75.8, 61.0, 56.1, 56.0, 31.9, 31.8, 10.2, 10.1. HRESIMS m/z 399.1773 $[\text{M}+\text{Na}]^+$ (calc. for $\text{C}_{21}\text{H}_{28}\text{NaO}_6$ 399.1778).

2.9. 1-(3,4-Dimethoxy-5-(2-methoxy-4-(2-oxopropyl)phenoxy)phenyl)propan-2-one (**20**)

A vial charged with a mixture of PdCl_2 (1.0 mg, 0.0073 mmol), CuCl (7.2 mg, 0.073 mmol) and DMF/ H_2O 7:1 (100 μL) was stirred under an oxygen atmosphere (1 atm) for 1 h. **2** (25 mg, 0.073 mmol) was added and the solution was stirred for 16 h. 1 M HCl (1 mL) was added and the product was extracted with EtOAc (3×1 mL). The organic layers were combined and washed successively with sat. NaHCO_3 (1 mL), brine (1 mL) and dried over MgSO_4 . After concentration under reduced pressure, the crude product was purified by flash chromatography (petroleum ether/EtOAc gradient 8:2, 7:3 and 1:1 v/v) to afford **20** (12.8 mg, 0.034 mmol, 47%) as a yellow oil; ^1H NMR (CDCl_3) δ_{H} 6.83 (1H, d, $J = 8.1$ Hz), 6.80 (1H, d, $J = 1.9$ Hz), 6.71 (1H, dd, $J = 8.1$ and 1.9 Hz), 6.49 (1H, d, $J = 1.9$ Hz), 6.30 (1H, d, $J = 1.9$ Hz), 3.87 (6H, s), 3.83 (3H, s), 3.67 (2H, s), 3.54 (2H, s), 2.18 (3H, s), 2.11 (3H, s). ^{13}C NMR (CDCl_3) δ_{C} 206.5, 206.2, 153.8, 150.7, 150.5, 144.8, 138.9, 130.2, 129.7, 121.8, 119.5, 113.6, 112.5, 108.2, 61.0, 56.1, 56.0, 50.9, 50.7, 29.3, 29.1. HRESIMS m/z 395.1468 $[\text{M}+\text{Na}]^+$ (calc. for $\text{C}_{21}\text{H}_{24}\text{NaO}_6$ 395.1465).

2.10. 1-(4-(5-(2-Hydroxypropyl)-2,3-dimethoxyphenoxy)-3-methoxyphenyl)propan-2-ol (**21**)

To a solution of **20** (12.0 mg, 0.032 mmol) in MeOH (100 μL) was added NaBH_4 (3.0 mg, 0.083 mmol) and the reaction was stirred for 40 min at room temperature. The reaction was diluted with water (1 mL), and the product was extracted with EtOAc (3×1 mL). The combined organic layers were washed with HCl (1 mL, 10% aq.), brine (1 mL), dried over MgSO_4 and concentrated to afford **21** (9.6 mg, 0.025 mmol, 80%, unassigned mixture of stereoisomers) as a yellow oil; ^1H NMR (CDCl_3) δ_{H} 6.78–6.74 (2H, m), 6.65 (1H, dd, $J = 8.1$ and 1.9 Hz), 6.45 (1H, d, $J = 1.9$ Hz), 6.22 (1H, d, $J = 1.9$ Hz), 4.07–3.98 (1H, m), 3.88–3.83 (1H, m), 3.81 (3H, s), 3.81 (3H, s), 3.77 (3H, s), 2.71 (1H, dd, $J = 13.6$ and 4.5 Hz), 2.62–2.55 (2H, m), 2.45 (1H, dd, $J = 13.6$ and 8.3 Hz), 1.20 (3H, d, $J = 6.2$ Hz), 1.13 (3H, d, $J = 6.2$ Hz). ^{13}C NMR (CDCl_3) δ_{C} 153.7, 150.6, 150.6, 144.3, 138.4, 134.6, 134.0, 121.6, 119.6, 113.8, 111.9, 108.1, 68.8, 68.7, 61.0, 56.1, 56.0, 45.7, 45.5, 22.8, 22.6. HRESIMS m/z 399.1776 $[\text{M}+\text{Na}]^+$ (calc. for $\text{C}_{21}\text{H}_{28}\text{NaO}_6$ 399.1778).

2.11. 3-(4-Formyl-2-methoxyphenoxy)-4,5-dimethoxybenzaldehyde (**24**)

To a solution of **22** (42 mg, 0.123 mmol) in 1,4-dioxane (1 mL) and H_2O (200 μL) was added 2,6-lutidine (58 μL , 0.492 mmol), NaIO_4 (210 mg, 0.984 mmol) and OsO_4 (32 μL , 4.0 wt % in H_2O , 0.005 mmol). The reaction was stirred for 4 h at room temperature and then quenched with aq. Na_2SO_3 (1 mL) and EtOAc (4×1 mL). The combined organic layers were washed with 1 M HCl (1 mL), dried over MgSO_4 and concentrated *in vacuo* to afford **24** (26.7 mg,

0.084 mmol, 70%) as a yellow oil; ^1H NMR (CDCl_3) δ_{H} 9.90 (1H, s), 9.80 (1H, s), 7.53 (1H, d, $J = 1.8$ Hz), 7.39 (1H, dd, $J = 8.2$ and 1.8 Hz), 7.31 (1H, d, $J = 1.8$ Hz), 7.11 (1H, d, $J = 1.8$ Hz), 6.88 (1H, d, $J = 8.2$ Hz), 3.96 (3H, s), 3.95 (3H, s), 3.93 (3H, s). ^{13}C NMR (CDCl_3) δ_{C} 190.9, 190.3, 154.3, 151.4, 150.6, 148.8, 146.0, 132.7, 131.8, 125.7, 117.3, 116.2, 110.7, 107.7, 61.3, 56.4, 56.2. HRESIMS m/z 317.1020 $[\text{M}+\text{Na}]^+$ (calc. for $\text{C}_{17}\text{H}_{17}\text{O}_6$ 317.1020).

2.12. General bioassays procedures

BALB/c mice were obtained from the animal breeding facility at the Instituto Adolfo Lutz, Brazil. The animals were maintained in sterilized cages under a controlled environment, and received water and food *ad libitum*. All procedures performed were previously approved by the Animal Care and Use Committee from Instituto Adolfo Lutz – Secretary of Health of Sao Paulo State (Project number CEUA 04/2016) in agreement with the Guide for the Care and Use of Laboratory Animals from the National Academy of Sciences.

2.13. Parasites and mammalian cell maintenance

Macrophages were collected from the peritoneal cavity of BALB/c mice by washing them with RPMI-1640 medium supplemented with 10% fetal calf serum, and were maintained at 37 °C in a 5% CO_2 humidified incubator. Trypomastigotes of *T. cruzi* (Y strain) were maintained in Rhesus monkey kidney cells (LLC-MK2 - ATCC CCL 7), cultivated in RPMI-1640 medium supplemented with 2% fetal calf serum at 37 °C in 5% CO_2 humidified incubator. The murine conjunctive cells (NCTC clone 929, ATCC) were maintained in RPMI-1640 supplemented with 10% FBS at 37 °C in a humidified atmosphere containing 5% CO_2 .

2.14. Determination of the 50% inhibitory concentration (IC_{50})

2.14.1. Extracellular forms

Trypomastigotes were counted in a hemocytometer chamber and seeded at 1×10^6 cells per well in 96 well microplates. The compounds were dissolved in DMSO and diluted in RPMI-1640 medium and incubated for 24 h at 37 °C in a 5% CO_2 humidified incubator. The parasite viability was determined using the resazurin (0.011% in PBS). The optical density was read at 570 nm using control wells without drugs (100% viability) and without cells (blank). The control group consisted of trypomastigotes incubated with 0.5% (v/v) DMSO. Benznidazole was used as a positive control. Compounds were tested to the highest concentration of 30 μM and were reported as NA (not active) when the IC_{50} value was above this concentration.

2.14.2. Intracellular amastigotes

Peritoneal macrophages were dispensed (1×10^5 /well) in 16 well chamber slides (NUNC, Thermo, USA) and maintained for 24 h in the same medium at 37 °C in a 5% CO_2 humidified incubator for attachment. Non-adherent cells were removed by two step washings with medium. After 24 h, these cells were infected with 5×10^5 culture trypomastigotes for 4 h. Benznidazole was used as the standard drug. Subsequently, infected cells were incubated with the compounds for 48 h. Finally, the slides were fixed with methanol, stained with Giemsa, and observed in light microscopy (100X magnification). The parasite load was defined by the number of infected macrophages X number of intracellular amastigotes/number of total macrophages.

2.15. Cytotoxicity in mammalian cells

The murine conjunctive cells (NCTC clone 929, ATCC) were counted in a hemocytometer chamber, seeded at 6×10^4 /well and incubated in highest concentrations to 200 μM for 48 h at 37 °C in a 5% CO_2 humidified incubator. The cell viability was determined using the MTT assay. Benznidazole was used as a positive control. The selectivity index (SI) was determined using the relationship, CC_{50} against NCTC/ IC_{50} against amastigotes parasites.

2.16. Evaluation of plasma membrane permeability

Late growth-phase trypomastigotes of *T. cruzi* (2×10^6 /well) were washed and incubated in the dark with 1 μM SYTOX Green probe (Molecular Probes) in HANKS' balanced salts solution (HBSS; Sigma-Aldrich) supplemented with 10 mM D-Glucose (HBSS + Glu). The test compound was added ($t = 0$) at the IC_{50} and fluorescence was measured every 20 min for 1 h. The maximum permeabilization was obtained with 0.5% Triton X-100. Fluorescence intensity was determined using a fluorimetric microplate reader (FilterMax F5 Multi-Mode Microplate Reader-Molecular Devices) with excitation and emission wavelengths of 485 and 520 nm, respectively. The following internal controls were used in the evaluation: i) the background fluorescence of the compound at the respective wavelengths, ii) the possible interference of DMSO. Samples were tested in duplicate [19].

2.17. Assessment of plasma membrane electric potential ($\Delta\Psi_p$)

Estimation of $\Delta\Psi_p$ was monitored by measuring the increase in absorbance of bis-(1,3-diethylthiobarbituric acid) trimethineoxonol [DiSBAC₂(3)] (Invitrogen) as described by Ref. [19]. Briefly, trypomastigotes of *T. cruzi* (2×10^6) were washed with HBSS + Glc, added into flow cytometry tubes and treated with compound **14** (IC_{50}) in a final volume of 150 μL and incubated at 37 °C for 60 min. Next, 0.2 μM of DiSBAC₂(3) were added in a final volume of 500 μL /tube and incubated at 37 °C for 10 min. The samples were read in an Attune NxT Flow Cytometer (Thermo Fisher Scientific). Gramicidin D (0.5 $\mu\text{g}/\text{mL}$) (Sigma-Aldrich) was used as a positive control. Untreated parasites were used as negative controls. Two independent experiments were performed, each one with duplicate samples.

2.18. Evaluation of mitochondrial membrane potential ($\Delta\psi_m$)

Late growth-phase trypomastigotes of *T. cruzi* (2×10^6 /well) were treated with the test compound at the IC_{50} in HBSS + Glu during 2 h incubation at 37 °C. After incubation, parasites were washed and co-stained with JC-1 (0.3 $\mu\text{g}/\text{mL}$) for 10 min under the absence of light at 37 °C in order to monitor the mitochondrial membrane potential ($\Delta\psi_m$) and cell viability, respectively. Flow cytometry was performed using an Attune NxT Acoustic Focusing Cytometer (ThermoFisher Scientific) by analyzing 10,000 gated events using forward/side scatter (FSC/SSC), JC-1 fluorescence (BL1-A, filter 530/30 nm), PI fluorescence (BL2-A, filter 574/26 nm) and Attune Nxt[®] software included with the equipment. Unstained, JC-1-stained (untreated) parasites were used to set background fluorescence and compensation. Trypomastigotes treated with CCCP (10 μM) and untreated were used to obtain maximal and minimal mitochondrial depolarization, respectively [20].

2.19. Statistical analysis

The determination of the CC_{50} and IC_{50} values was obtained from sigmoid dose-response curves. The statistical significance (p value) between the samples was evaluated through the One-way

ANOVA method using the Tukey's Multiple Comparison test. All analyzes were performed using Graph Pad Prism 5.0 software. The samples were tested in duplicate or triplicate and the assays were repeated at least twice.

3. Results

3.1. Preparation of semi-synthetic derivatives 3–25 from natural compounds 1 and 2

Natural products **1** and **2** present a number of sites that permit synthetic modification, including the phenol residue in the case of compound **1**, and the two unsaturated allyl side chains. The modifications selected were designed with several purposes in mind: to discover where potential exists for structural diversification without compromising bioactivity, to investigate derivatives that are easily accessible from the natural products, and to explore modifications that would address potential pharmacological concerns. Targeted modifications included transformations of the aryl ethers and phenols, double bond functionalization (such as hydrogenation, addition of heteroatoms, and oxidation). The synthetic routes employed to access the 23 derivatives studied in this work are shown in Figs. 2 and 3.

3.2. In silico analysis of semi-synthetic derivatives

In silico predictions of drug safety and physicochemical properties associated with clinical success were performed for the semi-synthetic library (compounds **3–25**) using FAF-Drugs4 web server [21]. This analysis includes multiple predictive models including the Lilly MedChem Rules, phospholipidosis, aqueous solubility, and oral property space prediction. The series was predicted to have good oral bioavailability based on a comparison of 15 physicochemical descriptors of oral drugs. In general, the series has higher lipophilicity than optimal, which may result in low aqueous

solubility and a higher probability of exhibiting toxicity. No analogs were identified as potential Pan Assay Interference (PAINS) compounds based on the three available filters; nor is the series predicted to induce phospholipidosis. Compound **14**, which proved promising in bioassays has good predicted oral bioavailability based on the VeberRules, Egan Rules, and Bayer Oral Property Space Rules, despite not meeting Lipinski's R05. Overall, *in silico* analysis indicated the primary risks for the series are associated with high lipophilicity, which could in the future be addressed by structural modifications that decrease lipophilicity.

3.3. In vitro efficacy and cytotoxicity

Twenty-three neolignan derivatives (compounds **3–25**) were prepared and tested *in vitro* against *T. cruzi* trypomastigotes and intracellular amastigotes, using the colorimetric resazurin assay and light microscopy counting, respectively. Among them, eight compounds (**5**, **8**, **12–14**, **16**, **22**, and **25**) showed activity against the intracellular amastigotes, with IC₅₀ values between 7 and 16 μM; five compounds (**3**, **14–16**, and **18**) demonstrated activity against trypomastigotes, with IC₅₀ values between 8 and 64 μM (Table 1). Two compounds (**14** and **16**) exhibited activity against both forms of the parasite. Among the twenty-three compounds, eighteen presented no mammalian cytotoxicity (NCTC cells) to the highest tested concentration of 200 μM, while five derivatives (**3**, **14–17**), demonstrated CC₅₀ values between 58.0 and 156.0 μM. Benznidazole was used as standard, giving IC₅₀ values of 17.7 ± 1.9 μM against trypomastigotes and 5.0 ± 1.5 μM against intracellular amastigotes.

Additionally, light microscopy images of *T. cruzi*-infected macrophages (Fig. 4A), demonstrated that compound **14** eliminated 100% of intracellular amastigotes, without affecting the morphology of host cells at the highest tested concentration of 30 μM (Fig. 4B).

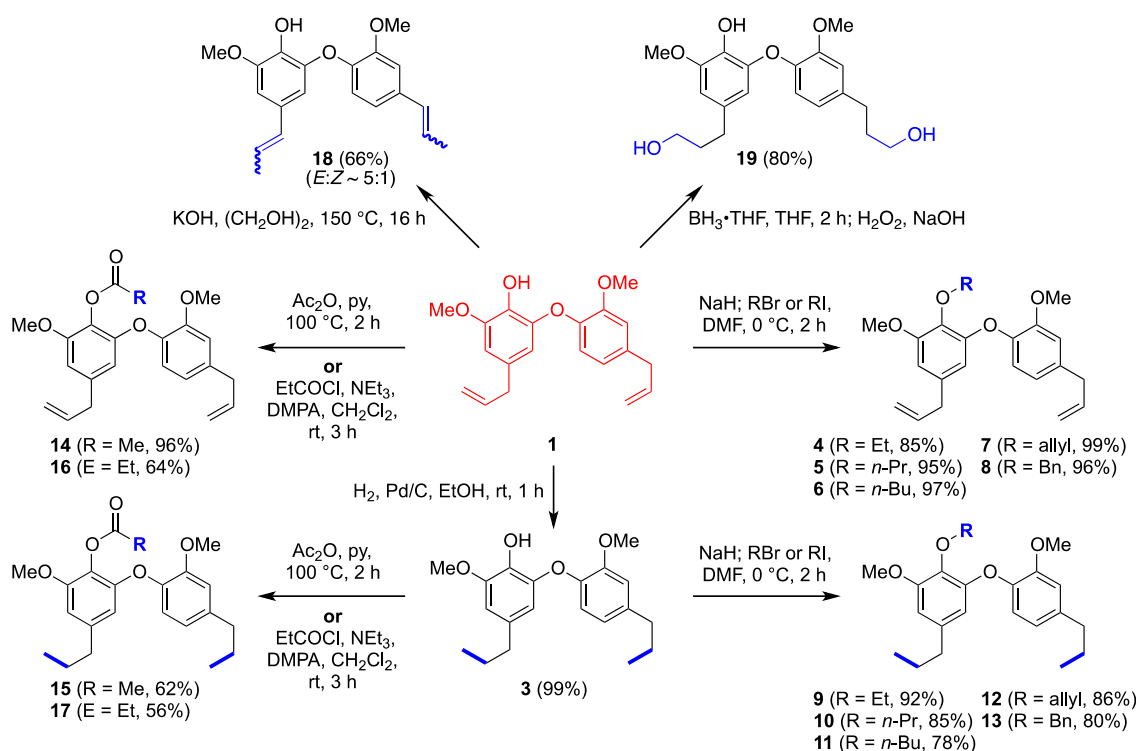


Fig. 2. Conversion of dehydrodieugenol B (**1**) to derivatives **3–19**.

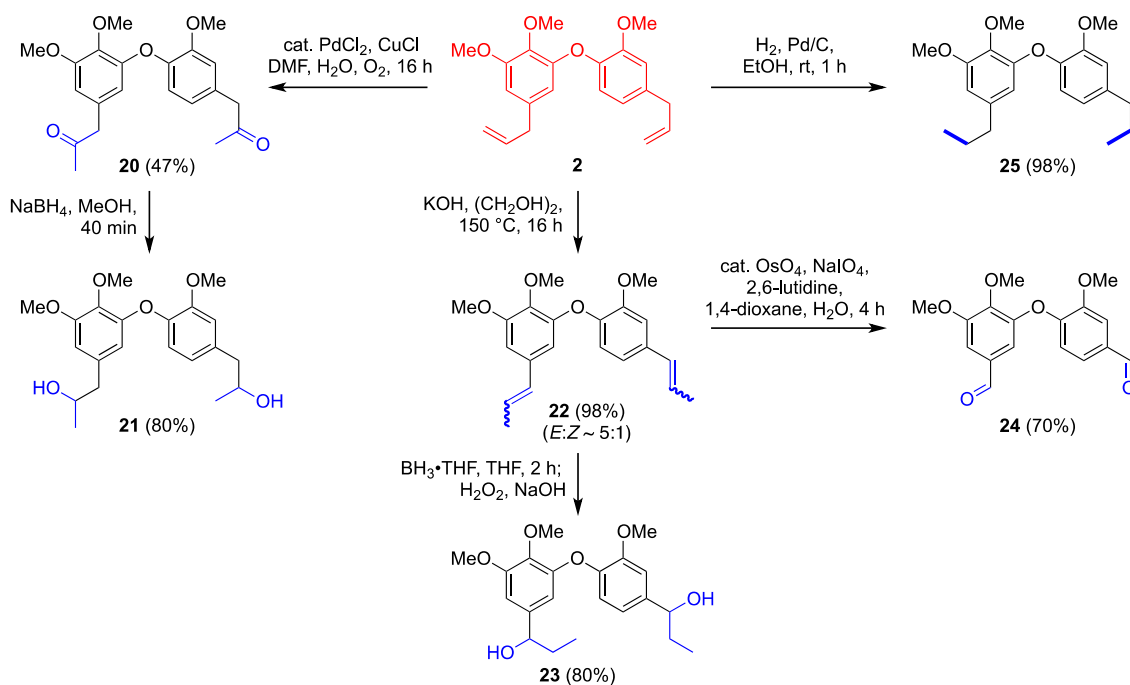


Fig. 3. Conversion of methyl dehydrodieugenol B (2) to derivatives 20–25.

Table 1

Anti-*T.cruzi* activity (trypomastigote and amastigote forms) and mammalian cytotoxicity (NCTC cells) of natural compounds **1** and **2**, semisynthetic derivatives **3**–**25** and benznidazole.

compound	IC ₅₀ (μM) (±S.D.)		CC ₅₀ (μM) (±S.D.) NCTC	S.I. amastigotes
	trypomastigotes	amastigotes		
1	38.6 ± 8.3	86.5 ± 16.2	>200	>2.3
2	>100	>30	>200	–
3	7.9 ± 0.7	>30	57.7 ± 1.1	–
4	>100	>30	>200	–
5	>100	16.4 ± 0.4	>200	>12.2
6	>100	>30	>200	–
7	>100	>30	>200	–
8	>100	9.5 ± 1.3	>200	>21.1
9	>100	>30	>200	–
10	>100	>30	>200	–
11	>100	>30	>200	–
12	>100	9.4 ± 3.9	>200	>21.2
13	>100	7.5 ± 1.1	>200	>26.6
14	64.2 ± 8.2	8.0 ± 5.8	64.4 ± 4.2	8.1
15	21.5 ± 2.9	>30	66.3 ± 6.0	–
16	30.5 ± 10.4	10.0 ± 0.8	75.0 ± 13.8	7.5
17	>100	>30	156.1 ± 15.0	–
18	26.6 ± 5.3	>30	>200	–
19	>100	>30	>200	–
20	>100	>30	>200	–
21	>100	>30	>200	–
22	>100	12.2 ± 3.5	>200	>16.4
23	>100	>30	>200	–
24	>100	>30	>200	–
25	>100	13.3 ± 1.2	>200	>15.4
benznidazole	17.7 ± 1.9	5.0 ± 1.5	190.6 ± 13.4	38.1

IC₅₀: 50% Inhibitory Concentration; CC₅₀: 50% Cytotoxic Concentration; S.I.: Selectivity Index, given by the ratio between CC₅₀ in NCTC cells and IC₅₀ in intracellular amastigotes; S.D.: Standard Deviation.

3.4. Mechanism of action studies

3.4.1. Plasma membrane permeability. In light of the *in vitro* potency of compound **14** and its capacity to eliminate 100% of parasites, its plasma membrane permeability was investigated using the fluorescent probe SYTOX Green. **14** induced no significant alteration

in plasma membrane permeability within 60 min of incubation when compared to untreated parasites (Fig. 5A). Triton X-100 was used as the positive control and was also included at the end of the assay to all groups. **14** was also incubated with macrophages, and the fluorescence monitored for 60 min. When compared to the untreated control, **14** showed no alteration of plasma membrane

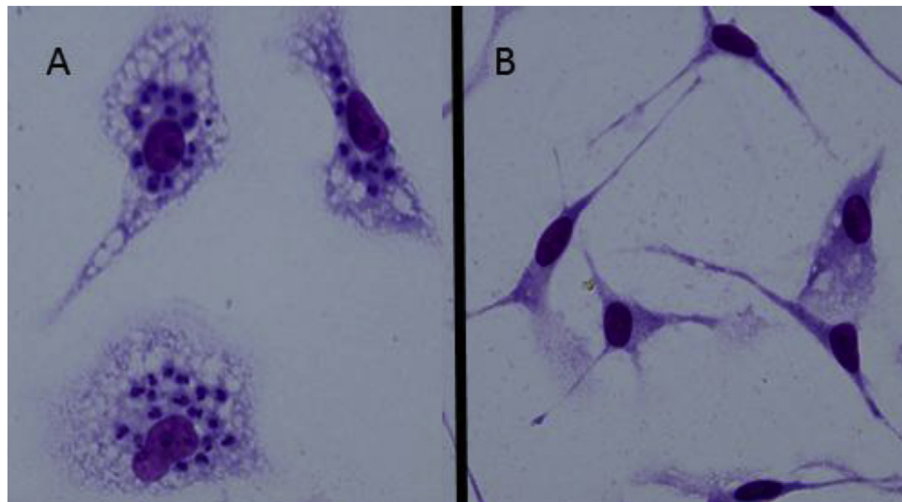


Fig. 4. Treatment of *Trypanosoma cruzi*-infected macrophages with compound **14**. Light microscopy images of Giemsa-stained slides. **A.** Untreated group with intracellular amastigotes. **B.** Group treated with compound **14** for a period of 48 h at 30 μ M. Magnification 100X (oil immersion).

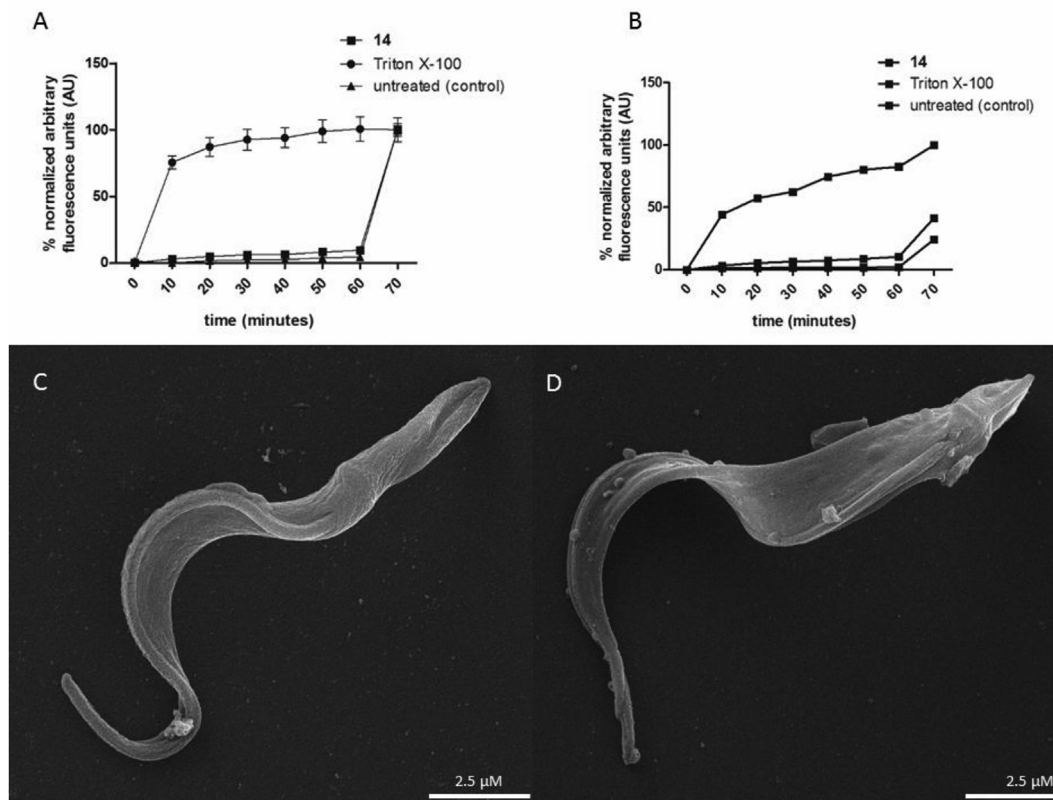


Fig. 5. Evaluation of the plasma membrane of *T. cruzi* trypomastigotes. SYTOX Green assay for the determination of the plasma membrane permeability of trypomastigotes (**A**) and peritoneal macrophages (**B**), both treated with compound **14**. Triton X-100 was used as the 100% of permeabilization (positive control) and a control group (untreated) was also included for both cells. **C.** Scanning electron microscopy *T. cruzi* untreated trypomastigotes (control group). **D** Scanning electron microscopy *T. cruzi* **14**-treated trypomastigotes (bar = 2.5 μ m).

permeability (Fig. 5B). Scanning electron microscopy studies of trypomastigotes incubated with **14** corroborated the SYTOX Green assay, as demonstrated by the normal morphology of *T. cruzi* trypomastigotes, including the plasma membrane of treated parasites (Fig. 5D), when compared to untreated group (Fig. 5C).

3.4.2. Plasma membrane electric potential ($\Delta\Psi_p$). Using flow cytometry analysis, the electric potential of plasma membrane of

T. cruzi trypomastigotes was investigated in the presence of compound **14**. After 60 min incubation, no significant alteration was observed when compared to untreated control (Fig. 6). Gramicidin, (a commercial antibacterial polypeptide) was used as positive control, and induced the depolarization of potential as shown in Fig. 6.

3.4.3. Mitochondrial membrane potential ($\Delta\Psi_m$). The capacity of

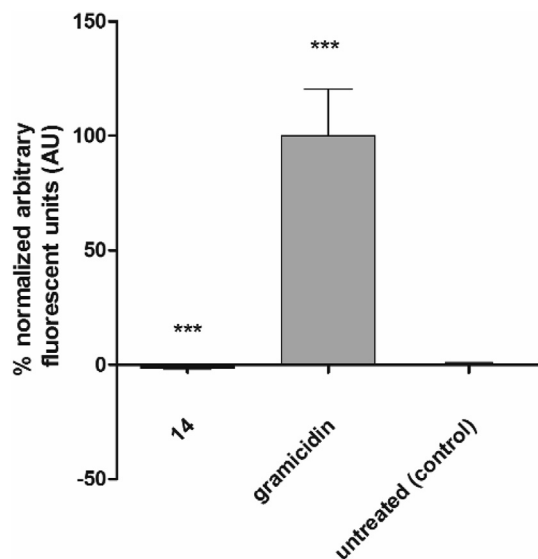


Fig. 6. Evaluation of the plasma membrane electric potential ($\Delta\Psi_p$) of *T. cruzi* trypomastigotes treated with compound 14. DiSBAC2 (3) dye ($0.2\ \mu\text{M}$) fluorescence was measured in a flow cytometer (ATTUNE). Minimum (untreated) and maximum (gramicidin – $0.5\ \text{mg/mL}$) alteration in the electric potential permeabilization were obtained. Fluorescence was quantified by calculating the mean percentages of untreated (0%) and gramicidine-treated (100%) parasites. $^{**}p < 0.005$.

compound **14** to affect the mitochondria of *T. cruzi* trypomastigotes was investigated using flow cytometry. Initially, the mitochondrial membrane potential was studied in the presence of the fluorescent probe JC-1. After 120 min of incubation, compound **14** induced a significant ($p < 0.05$) reduction of fluorescence levels when compared to untreated parasites, resulting in the depolarization of the mitochondrial membrane (Fig. 7). Carbonyl cyanide-*m*-chlorophenylhydrazone (CCCP) was used as a positive control at $50\ \mu\text{M}$ and caused a significant depolarization of mitochondria when compared to untreated cells.

3.4.1. ROS levels

The levels of reactive oxygen species in trypomastigotes were

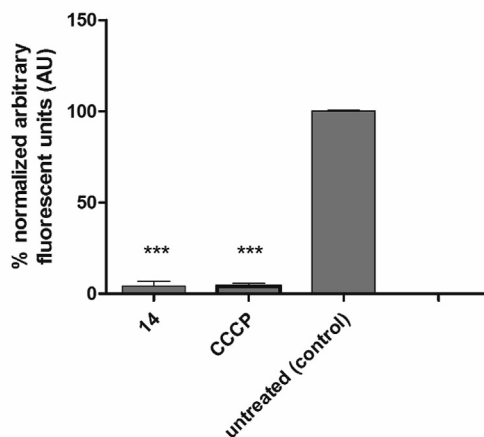


Fig. 7. Evaluation of the mitochondrial membrane potential of *T. cruzi* trypomastigotes incubated with compound **14**. Changes of JC-1 fluorescence determined by flow cytometry (ATTUNE) and reported as normalized data based in untreated parasites. Maximal and minimal fluorescence of JC-1 were achieved by non-treatment and treatment with CCCP ($50\ \mu\text{M}$). Trypomastigotes were treated at the IC_{50} value of compound 14 for 2 h $^{***}p < 0.005$ related to positive control (CCCP).

determined using the fluorescent probe $\text{H}_2\text{DCF-DA}$. Compound **14** induced significant ($p < 0.05$) reduction in ROS levels after treatment for 120 min when compared to untreated parasites. Sodium azide was used as a positive control (Fig. 8).

3.5. SAR trends for optimization studies

Based on the *T. cruzi* activity of the phenolic natural product dehydrodieugenol B (**1**) and lack of activity and cytotoxicity for the corresponding natural methyl derivative (**2**) we hypothesized that the phenol is important for *T. cruzi* activity but is also associated with cytotoxicity. While many molecules such as flavonoids and other related compounds feature phenols [22], these motifs can be associated with toxicity profiles [23,24]; substituted phenols can form phenoxy radicals or toxic metabolites such as quinones, and are therefore of concern for drug discovery [25]. To evaluate whether the phenol is required for activity against *T. cruzi*, the library of semi-synthetic analogs was evaluated for anti-trypomastigote activity and cytotoxicity against NCTC cells. Notably, compounds lacking the free phenol exhibited activity against intracellular amastigotes, and all exhibited greater potency compared to the natural product **1**, particularly for ether derivatives. All semi-synthetic ether analogs containing allyl side chains (compounds **4–8**) exhibited no mammalian cytotoxicity to the maximal tested concentration ($>200\ \mu\text{M}$). Two analogs – propyl ether **5** ($\text{IC}_{50} = 16.4 \pm 0.4\ \mu\text{M}$) and benzyl ether **8** ($\text{IC}_{50} = 9.5 \pm 1.3\ \mu\text{M}$) – were more potent against *T. cruzi* amastigotes than **1** ($\text{IC}_{50} = 86.5 \pm 16.3\ \mu\text{M}$). Phenolic esters exhibited further improvement of *T. cruzi* intracellular amastigote potency, but a slight erosion of selectivity compared to ether analogs **5** and **8**. Despite the decreased selectivity of esters compared to ethers, esters **14** and **16** overall exhibited improved selectivity index values (8.0 and 7.5, respectively) compared to natural product **1** (>2.3). It was concluded that the phenol may not be required for activity in *T. cruzi* amastigotes, but is likely to play a role in mammalian cytotoxicity. Interestingly, esters **14** and **16** exhibited activity against both forms of the parasite, unlike the ether analogs.

In light of this dual bioactivity, compound **14** was selected for further evaluation against both the amastigote and trypomastigotes forms of the parasite. Of concern was its metabolic susceptibility to

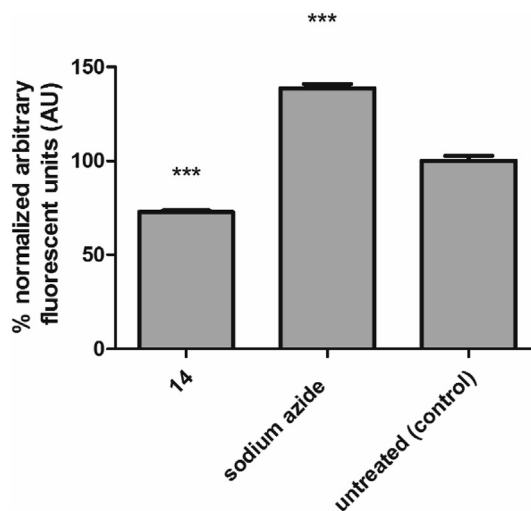


Fig. 8. Production of reactive oxygen species (ROS) in *T. cruzi* trypomastigotes incubated with compound **14**. $\text{H}_2\text{DCF-DA}$ was incubated with the cells, and the fluorescence intensity was detected using a fluorimetric microplate reader (FilterMaxF5 Multi-Mode Microplate Reader) with excitation and emission wavelengths of 485 and 520 nm, respectively. Azide ($10\ \mu\text{M}$) was used as positive control. $^{***}p < 0.001$.

hydrolysis, which would result in *in situ* formation of compound **1**. Indeed, esters are often used as pro-drugs to increase solubility or permeability, and are hydrolyzed *in vivo* to the corresponding alcohols [26]. One potential explanation for the increased *T. cruzi* activity could be that the acetylated derivative **14** achieves greater intracellular and intra-parasitic concentrations compared to **1**, and it is subsequently hydrolyzed to the phenol-containing natural product **1**. By comparison, ethers are typically more metabolically stable than esters with respect to hydrolysis; the activity of ethers **5** and **8** may therefore suggest that the phenol is not required for *T. cruzi* activity, but may be beneficial.

In contrast, the allyl sidechains appear to play a key role in *T. cruzi* activity, especially against intracellular forms. Reduction of allyl ethers (**12** and **13** - IC_{50} 9.4 ± 3.9 and 7.5 ± 1.1 μ M, respectively) completely suppressed *T. cruzi* amastigote and trypomastigote activity in the resulting saturated ether analogs **9–11**. Likewise, reduction of ester analogs (**14** and **16**) to saturated ester analogs (**15** and **17**) completely suppressed amastigote activity. Interestingly, the saturated trimethoxyl compound, **25**, exhibits improved amastigote activity compared to the corresponding allyl analog, **2**, which is inactive (IC_{50} 13.3 ± 11.2 μ M ($SI > 15$) and >30 μ M, respectively).

Analogs replacing the allylic groups with hydrogen bond donating (HBD) and accepting (HBA) groups (compounds **19–21**, **23** and **24**) resulted in loss of activity against *T. cruzi* amastigotes, and no toxicity against NCTC cells. Interestingly, methyl ether **22** (featuring internal *E*-olefins) was active against *T. cruzi* amastigotes with an IC_{50} value of 12.2 ± 3.5 μ M. However, the corresponding phenol **18** was not active against amastigotes. Overall, these studies of the allyl sidechains suggest that the scaffold is tolerant of structural modifications, and indeed modifications can improve *T. cruzi* amastigote activity, and selectivity against mammalian cells.

4. Discussion

Previous studies from our groups demonstrated the anti-trypansomal activity of the natural products dehydrodieugenol B (**1**) and methyldehydrodieugenol B (**2**), isolated from the plant *N. leucantha* [17]. Compound **1**, was found to be effective against *T. cruzi*, with an IC_{50} value of 86.5 μ M (intracellular amastigotes) and 38.6 μ M (trypomastigotes) and no toxicity against NCTC cells observed. *In silico* studies suggested that compounds **1** and **2** are not likely to exhibit pan-assay interference (PAINS), and have low risk of carcinogenic, mutagenic or genotoxic activity [17]. In the present work, we targeted the semi-synthetic modification of natural products **1** and **2** to obtain a series of derivatives that would explore the importance and modification potential of the phenol and allyl sidechains, and which might lead to analogs with better potency against *T. cruzi*, and improved selectivity indices compared to mammalian cells.

Twenty-three semi-synthetic neolignan derivatives were prepared, and studied for their bioactivity against the extracellular trypomastigote and intracellular amastigote forms of *T. cruzi*, and for cytotoxicity towards murine fibroblasts (NCTC cells). For *T. cruzi*, the intracellular amastigote form is the most clinically relevant, but the trypomastigote form is also found in mammals in the acute phase of the disease, and can result in reactivation of the parasitaemia. As such, drugs that selectively affect trypomastigotes are also considered a relevant therapeutic approach [27].

In terms of the allyl sidechains, this semi-synthetic approach modified both sidechains simultaneously and equivalently; at this early stage of investigation, no attempt was made to achieve selectivity, chemoselectivity or stereoselectivity. The discovery of promising bioactivity in such derivatives would be followed by a more in-depth analysis. As such, these investigations were

designed to probe whether semi-synthetic derivatives obtained directly from the natural products might have the potential for further synthetic optimizations.

Among the twenty-three derivatives, compounds **13** and **14** showed the highest potency against amastigotes, with IC_{50} values close to the standard drug benznidazole. Compound **13** also demonstrated the highest selectivity index ($SI > 26$). However, only compound **14** (which displayed a similar potency to compound **16** against amastigotes) eliminated 100% of intracellular amastigotes, without affecting the morphology of host cells at the highest tested concentration. Masking of the phenol functional group as an ether consistently improved selectivity against mammalian cells; all ether analogs, including compound **13**, were not cytotoxic to mammalian NCTC cells at concentrations up to 200 μ M. Esterification of the phenol also decreased mammalian cytotoxicity, but to a lesser extent compared to the ether analogs.

Analysis of the bioactivity trends of the semi-synthetic neolignan library provides some information on the structure activity relationships (SARs) within the natural product scaffold, and identifies sites where future modifications might be tolerated. Our studies first reveal that at least one of the unsaturated side chains is important for *T. cruzi* activity, as the fully saturated derivatives **9–11** were inactive. However, the derivatives **12**, **13** and **25** featuring allyl, benzyl, and methyl ether substituents in place of the phenol of **1** retained good activity against amastigotes. In the former two cases, this may relate to an element of *pseudo*-symmetry in the natural product scaffold, such that the allyl ether of **12** serves as a surrogate for an allyl sidechain. Notably, the isomerized derivatives **18** and **22** retain good activity against the trypomastigote forms compared to their parent allyl sidechains. However, an expressive effect against intracellular amastigote forms was observed to compound **22**, which could be explained by the differences in intracellular concentrations due to permeability.

The phenol natural product **1** exhibits good activity and no significant toxicity in the mammalian cell assay. The corresponding esters **14** and **16** showed a considerable increase in potency compared to compound **1**, but similar toxicity, and thereby exhibit an improved selectivity index. Other modifications were less well tolerated. For example, all derivatives containing oxygenated sidechains (compounds **19–21**, **23**, and **24**) were inactive against both forms of the parasite, despite the increase in aqueous solubility that these compounds presumably exhibit. This suggests that at least one non-polar sidechain is required for the anti-trypansomal activity.

Considering the promising *in vitro* activity of compound **14**, this derivative was subjected to phenotypic analysis of drug-treated parasites, with the goal of identifying the major cellular targets involved in its antitrypanosomal action. Previous studies with a related neolignan also isolated from *N. leucantha* [17] indicated a strong permeabilization effect in the plasma membrane of *T. cruzi*, an effect that could also be the cause of mammalian cell toxicity. Interestingly, the new derivative **14** induced neither alterations in the plasma membrane of *T. cruzi* nor in the host macrophages, suggesting that the presence of an acetyl group instead of a methyl group alters its affinity towards the *T. cruzi* membrane. Scanning electron microscopy enabled us to visualize the unaltered nature of the plasma membrane, and the preserved parasite morphology, thus corroborating our fluorimetric permeability studies.

One potential explanation for the heightened activity of compound **14** is that the ester functionality facilitates membrane permeability, leading to a greater intracellular concentration of compound **1** (post-hydrolysis) in the macrophages and amastigotes. Furthermore, the poor bioactivity exhibited by many of the corresponding ether analogs (which are less likely undergo O-dealkylation) supports the notion that the phenol itself plays a key

role in the observed potency. The exception to this, as described above, are compounds **12** and **13** where further studies are required to elucidate the phenotypic mode of action.

In contrast to most eukaryotic cells, *T. cruzi* presents a single mitochondrion that displays unusual features, such as a specific arrangement of mitochondrial DNA (the kinetoplast). Due to this, Trypanosomatidae mitochondria have been identified as candidate target organelles for new drugs. Mitochondria are involved in cellular redox processes, playing a central role in energy metabolism through oxidative phosphorylation (resulting in ATP synthesis, calcium homeostasis, nutrient oxidation, and control of apoptosis) [28].

The mitochondrial membrane potential of *T. cruzi* was measured using flow cytometry after incubation with compound **14**, using the fluorescent probe JC-1. When compared to positive controls and untreated cells, a strong depolarization was observed after 2 h incubation. The mitochondrial membrane potential ($\Delta\Psi_m$) is the result of an electrochemical gradient and is critical for maintaining the physiological function of the respiratory chain to generate ATP. A significant loss of the $\Delta\Psi_m$ renders cells depleted of energy with subsequent death [29].

Mitochondria are also the main source of reactive oxygen species (ROS), regulated by the redox state of the electron transport system or the magnitude of the mitochondrial membrane potential [30]. At high levels, ROS can cause cellular damage, especially when cells cannot cope with this condition. In our studies, *T. cruzi* parasites treated with compound **14** exhibited reduced ROS levels, suggesting that the depolarization of the mitochondrial membrane potential may contribute to this imbalance. The lethal anti-trypanosomal effect of this new neolignan derivative may therefore be ascribed to mitochondrial impairment, but other studies of mechanism of action will be required to confirm this.

Acknowledgments

This work was funded by grants and fellowships provided from São Paulo State Research Foundation (FAPESP 2015/50075-2, 2018/10279-6, 2018/07885-1 and 2016/24524-7). We also thank Conselho Nacional de Pesquisa e Desenvolvimento scientific research award (CNPq to AGT and JHGL) and CAPES for the student's scholarships. CES is grateful to the EPSRC Centre for Doctoral Training in Synthesis for Biology and Medicine (EP/L015838/1) for a studentship, generously supported by AstraZeneca, Diamond Light Source, Defence Science and Technology Laboratory, Evotec, GlaxoSmithKline, Janssen, Novartis, Pfizer, Syngenta, Takeda, UCB and Vertex. EAA thanks the Oxford SPRINT Fund in collaboration with FAPESP, and EPSRC–GCRF for funding, and the EPSRC for additional support (EP/M019195/1).

Appendix A. Supplementary data

Supplementary data to this article can be found online at <https://doi.org/10.1016/j.ejmech.2019.05.001>.

References

- [1] C. Bern, Chagas' disease, *N. Engl. J. Med.* 373 (2015) 456–466, <https://doi.org/10.1056/NEJMr1410150>.
- [2] A. Rassi Jr., A. Rassi, J. Marcondes de Rezende, American trypanosomiasis (Chagas disease), *Infect. Dis. Clin. N. Am.* 26 (2012) 275–291, <https://doi.org/10.1016/j.idc.2012.03.002>.
- [3] G.A. Schmunis, Z.E. Yadon, Chagas disease: a Latin American health problem becoming a world health problem, *Acta Trop.* 115 (2010) 14–21, <https://doi.org/10.1016/j.actatropica.2009.11.003>.
- [4] J. Gascon, C. Bern, M.J. Pinazo, Chagas disease in Spain, the United States and other non-endemic countries, *Acta Trop.* 115 (2010) 22–27, <https://doi.org/10.1016/j.actatropica.2009.07.019>.
- [5] Y. Jackson, A. Pinto, S. Pett, Chagas disease in Australia and New Zealand: risks and needs for public health interventions, *Trop. Med. Int. Health* 19 (2014) 212–218, <https://doi.org/10.1111/tmi.12235>.
- [6] World Health Organization, Integrating Neglected Tropical Diseases into Global Health and Development: Fourth WHO Report on Neglected Tropical Diseases, 2017. Geneva.
- [7] Z.M. Cucunubá, O. Okuwoga, M.G. Basáñez, P. Nouvellet, Increased mortality attributed to Chagas disease: a systematic review and meta-analysis, *Parasites Vectors* 9 (2016) 42, <https://doi.org/10.1186/s13071-016-1315-x>.
- [8] R.B. Bestetti, A. Cardinalli-Neto, Did death hinder the process of justice? Carlos Chagas and the nobel prize of 1935, *Int. J. Cardiol.* 147 (2011) 172–173, <https://doi.org/10.1016/j.ijcard.2010.12.020>.
- [9] F.X. Lescurre, G. Le Loup, H. Freilij, M. Develoux, L. Paris, L. Brutus, G. Pialoux, Chagas disease: changes in knowledge and management, *Lancet Infect. Dis.* 10 (2010) 556–570, [https://doi.org/10.1016/S1473-3099\(10\)70098-0](https://doi.org/10.1016/S1473-3099(10)70098-0).
- [10] J. Bermudez, C. Davies, A. Simonazzi, J.P. Real, S. Palma, Current drug therapy and pharmaceutical challenges for Chagas disease, *Acta Trop.* 156 (2016) 1–16, <https://doi.org/10.1016/j.actatropica.2015.12.017>.
- [11] A.J. Romanha, S.L. Castro, M. de N. Soeiro, J. Lannes-Vieira, I. Ribeiro, A. Talvani, B. Bourdin, B. Blum, B. Olivieri, C. Zani, C. Spadafora, E. Chiari, E. Chatelain, G. Chaves, J.E. Calzada, J.M. Bustamante, L.H. Freitas-Junior, L.I. Romero, M.T. Bahia, M. Lotrowska, M. Soares, S.G. Andrade, T. Armstrong, W. Degraev, A.Z. de Andrade, *In vitro* and *in vivo* experimental models for drug screening and development for Chagas disease, *Mem. Inst. Oswaldo Cruz* 105 (2010) 233–238.
- [12] M.C. Campos, L.L. Leon, M.C. Taylor, J.M. Kelly, Benzimidazole-resistance in *Trypanosoma cruzi*: evidence that distinct mechanisms can act in concert, *Mol. Biochem. Parasitol.* 193 (2014) 17–19, <https://doi.org/10.1016/j.molbiopara.2014.01.002>.
- [13] S.R. Wilkinson, M.C. Taylor, D. Horn, J.K. Kelly, I. Cheeseman, A mechanism for cross-resistance to nifurtimox and benzimidazole in trypanosomes, *Proc. Natl. Acad. Sci. U. S. A.* 105 (2008) 5022–5027, <https://doi.org/10.1073/pnas.0711014105>.
- [14] D.J. Newman, G.M. Cragg, Natural products as sources of new drugs from 1981 to 2014, *J. Nat. Prod.* 79 (2016) 629–661, <https://doi.org/10.1021/acs.jnatprod.5b01055>.
- [15] S.S. Grecco, L. Lorenzi, A.G. Tempone, J.H.G. Lago, Update: biological and chemical aspects of *Nectandra* genus (Lauraceae), *Tetrahedron: Asymmetry* 27 (2016) 793–810, <https://doi.org/10.1016/j.tetasy.2016.07.009>.
- [16] T.A. da Costa-Silva, S.S. Grecco, F.S. de Sousa, J.H. Lago, E.G. Martins, C.A. Terrazas, S. Varikuti, K.L. Owens, S.M. Beverley, A.R. Satoskar, A.G. Tempone, Immunomodulatory and antileishmanial activity of phenylpropanoid dimers isolated from *Nectandra leucantha*, *J. Nat. Prod.* 78 (2015) 653–657, <https://doi.org/10.1021/np500809a>.
- [17] S.S. Grecco, T.A. Costa-Silva, G. Jerz, F.S. de Sousa, V.S. Londero, M.K. Galuppo, M.L. Lima, B.J. Neves, C.H. Andrade, A.G. Tempone, J.H.G. Lago, Neolignans from leaves of *Nectandra leucantha* (Lauraceae) display *in vitro* anti-trypanosomal activity via plasma membrane and mitochondrial damages, *Chem. Biol. Interact.* 277 (2017) 55–61, <https://doi.org/10.1016/j.cbi.2017.08.017>.
- [18] F.S. de Sousa, S.S. Grecco, N. Girola, R.A. Azevedo, C.R. Figueiredo, J.H.G. Lago, Neolignans isolated from *Nectandra leucantha* induce apoptosis in melanoma cells by disturbance in mitochondrial integrity and redox homeostasis, *Phytochemistry* 140 (2017) 108–117, <https://doi.org/10.1016/j.phytochem.2017.04.024>.
- [19] J.R. Luque-Ortega, L. Rivas, Characterization of the leishmanicidal activity of antimicrobial peptides, *Methods Mol. Biol.* 618 (2010) 393–420, https://doi.org/10.1007/978-1-60761-594-1_25.
- [20] R.M. Santa-Rita, A. Henriques-Pons, H.S. Barbosa, S.L. de Castro, Effect of the lysophospholipid analogues edelfosine, ilmofosine and miltefosine against *Leishmania amazonensis*, *J. Antimicrob. Chemother.* 54 (2004) 704–710.
- [21] D. Lagorce, O. Sperandio, H. Galons, M.A. Miteva, B.O. Villoutreix, FAF-Drugs2: free ADME/tox filtering tool to assist drug discovery and chemical biology projects, *BMC Bioinf.* 9 (2008) 396, <https://doi.org/10.1186/1471-2105-9-396>.
- [22] A.N. Panche, A.D. Diwan, S.R. Chandra, Flavonoids: an overview, *J. Nutr. Sci.* 5 (2016) e47, <https://doi.org/10.1017/jns.2016.41>.
- [23] M.Y. Moridani, A. Siraki, P.J. O'Brien, Quantitative structure toxicity relationships for phenols in isolated rat hepatocytes, *Chem. Biol. Interact.* 145 (2003) 213–223.
- [24] A.A. Shvedova, C. Kommineni, B.A. Jeffries, V. Castranova, Y.Y. Tyurina, V.A. Tyurin, E.A. Serbinova, J.P. Fabisiak, V.E. Kagan, Redox cycling of phenol induces oxidative stress in human epidermal keratinocytes, *J. Invest. Dermatol.* 114 (2000) 354–364.
- [25] H. Shadnia, J.S. Wright, Understanding the toxicity of phenols: using quantitative structure-activity relationship and enthalpy changes to discriminate between possible mechanisms, *Chem. Res. Toxicol.* 21 (2008) 1197–1204, <https://doi.org/10.1021/tx800058r>.
- [26] K. Hajnal, H. Gabriel, R. Aura, V. Erzsébet, S. Blanka, Prodrug strategy in drug development, *Acta Med. Marisiensis* 62 (2016) 356–362, <https://doi.org/10.1515/amma-2016-0032>.
- [27] K. Katsuno, J.N. Burrows, K. Duncan, R. Hooft van Huijsduijnen, T. Kaneko, K. Kita, C.E. Mowbray, D. Schmatz, P. Warner, B.T. Slingsby, Hit and lead criteria in drug discovery for infectious diseases of the developing world, *Nat. Rev. Drug Discov.* 14 (2015) 751–758, <https://doi.org/10.1038/nrd4683>.
- [28] R.F. Menna-Barreto, S.L. de Castro, The double-edged sword in pathogenic

- trypanosomatids: the pivotal role of mitochondria in oxidative stress and bioenergetics, *BioMed Res. Int.* 2014 (2014) 614014, <https://doi.org/10.1155/2014/614014>.
- [29] A.G. Tempone, D.D. Ferreira, M.L. Lima, T.A. Costa Silva, S.E.T. Borborema, J.Q. Reimão, M.K. Galuppo, J.M. Guerra, A.J. Russell, G.M. Wynne, R.Y.L. Lai, M.M. Cadelis, B.R. Copp, Efficacy of a series of alpha-pyrone derivatives against *Leishmania(L.) infantum* and *Trypanosoma cruzi*, *Eur. J. Med. Chem.* 139 (2017) 947–960, <https://doi.org/10.1016/j.ejmech.2017.08.055>.
- [30] T.R. Figueira, M.H. Barros, A.A. Camargo, R.F. Castilho, J.C. Ferreira, A.J. Kowaltowski, F.E. Sluse, N.C. Souza-Pinto, A.E. Vercesi, Mitochondria as a source of reactive oxygen and nitrogen species: from molecular mechanisms to human health, *Antioxidants Redox Signal.* 18 (2013) 2029–2074, <https://doi.org/10.1089/ars.2012.4729>.